An Optimal Control Scheme for Single-Phase Grid-Connected Photovoltaic Inverter

Guangru Zhang
College of Information Science and Engineering, Northeastern University,
ShenYang110819, Liaoning Province, China
Email: zhangguangru890722@163.com

Dongsheng Yang, Ting Liu and Bo Hu
College of Information Science and Engineering, Northeastern University,
ShenYang110819, Liaoning Province, China
Yuhong Power Supply Bureau of Shenyang Power Supply Company,
ShenYang110141, Liaoning Province, China
Liaoning Electric Power Company Limited, ShenYang110006, Liaoning Province, China
Email: yangdongsheng@mail.neu.edu.cn
14974661@qq.com
dianlihubo@sina.com

***Abstract*— In this paper, an optimal control scheme for single-phase grid-connected photovoltaic inverter is proposed. Besides a nonlinear mathematical model of the inverter in the DQ rotating coordinate is constructed. In addition, the designed controller has weaker dependence on the parameters of the system by selecting the appropriate performance control matrix. The simulation works show that this method can achieve zero steady-state error, has a good dynamic and static response, and it ensures that the system is robust in the case of parameters variations and fluctuations.**

***Index Terms* — Photovoltaic, Grid Connected, Optimal Method, Nonlinear Control**

I. INTRODUCTION

There are more and more energy consumption along with the development of the current economic and society. However the rapid development has formed a very prominent contradiction with the deteriorating environment and the gradual depletion of fossil fuel, research and utilization of clean and renewable energy has become an inevitable trend and received more and more attention around the world [1]. Grid connected photovoltaic power generation is the most important use of solar energy in the form, so it becomes a big hot issue of the current industry and academic in domestic and international. Common single-phase grid-connected photovoltaic system is shown in Figure 1. The system is mainly composed by boost chopper circuit and single-phase inverter circuit. Wherein on one hand, the boost chopper circuit ensures the voltage of photovoltaic panels to rise to the desired single-phase inverter DC bus voltage, on the other hand, it ensure the MPPT operation of photovoltaic modules, and the literature [2-5] have made a lot of studies , then this paper is not necessary to focus on the content.

In order to obtain the net output current which has high quality and controllable power factor angle, a number of control methods have been proposed, such as proportional-integral control, hysteresis control, proportional resonant control, repetitive control, slide mode control and so on. Using the conventional PI control loop to implement grid-connected controlling is simple structure with good stability and easy to adjust the control parameters, but the current need track grid voltage dynamically. It is difficult to eliminate steady error and mediate PI parameters, so the overall effect is poor [6]. In [7], it points out that although the algorithm of hysteresis control is simple, easy to implement and has fast dynamic response characteristics, and the hysteresis width has a great impact on the switching frequency, power loss and control accuracy. The smaller the ring width, the higher precision of the control method, but it will lead increasing switching frequency and the loss, while hysteresis control can also make the switching frequency fluctuations. In [8], the ratio of the resonant control can eliminate the steady state error in the signal tracking process and it can also be used to eliminate a lot of times and network harmonics, but it cannot compensate for the phase angle and has a strong dependence on the parameter accuracy, and the gain in the non-fundamental frequency becomes very small. When the grid frequency fluctuates, harmonic suppression is poor and it is not easy to be implemented in engineering. Because of the non-linear characteristics of the inverter, the proposed methods in [6-10] are difficult to achieve perfect dynamic and static characteristics by linear approximation to design a controller [11]. Therefore, it is necessary to research the nonlinear control methods to control the photovoltaic inverter system to achieve better static and dynamic

doi:10.4304/jcp.9.2.380-387

characteristics. Synovial control as a nonlinear control in the photovoltaic inverter control has been widely used. Despite the synovial control has a wide stability margin, and the system has good dynamic response and strong robustness, there are shocks and steady-state error issues [12]. The repetitive control when applied to the photovoltaic inverter control system having a larger amplitude-frequency gain due to endometrial role in the rated frequency can be realized without static differential compensation, but the presence of the phase angle hysteresis problem and the poor dynamic response are pointed out in [13]. And new PI parallel improved method for repetitive control is proposed, but the improvement is limited and the research is conducted on off-grid inverter. In [14], it designs a nonlinear controller based on Lyapunov function, and it proves that it has global stability, good dynamic and static characteristics, but its computational complexity and difficult to implement. Using the optimal control method in switching power converter achieves a stable operation in a wide range when the system operates in a large fluctuation range and the controller has a strong follower performance, and it also improve the system dynamic performance significantly [15-16]. The optimal control of nonlinear systems generally look for objective functional performance indicators and obtain the minimum value of the objective function along all possible trajectories of the system, so this problem is usually considered to resolve partial differential equations for the Hamilton-Jacobi-Bellman, but solving Hamilton-Jacobi-Bellman is very difficult in most cases. However, it is not need to design the objective function by introducing a suitable Lyapunov control function to obtain the minimal value before designing the controller. On the contrary, it only needs the value of introduced objective function minimum. Therefore it overcomes the difficultly of solving Hamilton-Jacobi-Bellman of the optimal control method [17].

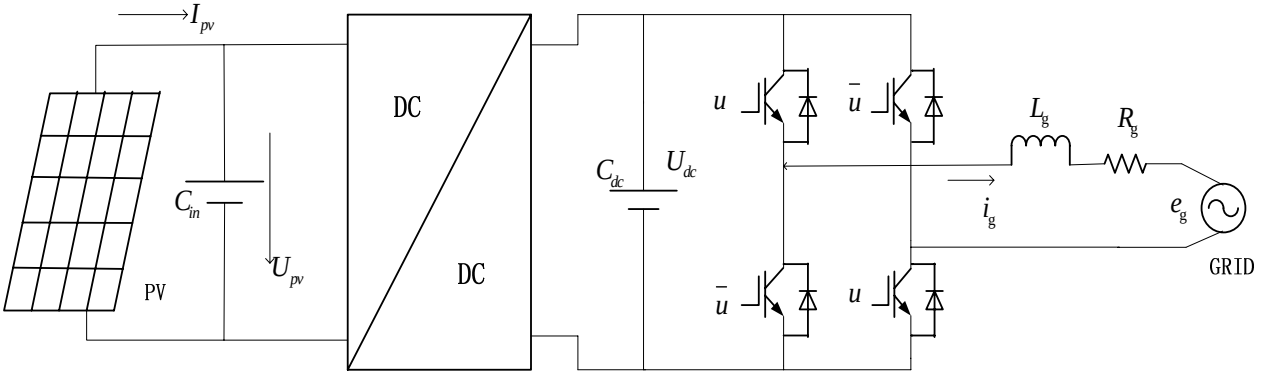

Fig 1 the Schematic of the Single-phase PV grid-connected

In this paper, the discrete optimal control method based on rotating coordinate for single-phase photovoltaic grid-connected control is proposed. On one hand, the construction of the nonlinear model for the single-phase grid-connected photovoltaic inverter realizes the control of the active and reactive power independently and this is also suitable for microprocessor digital implementation. On the other hand, simulation works indicate that the optimal control method ensures the strong robustness of the system in the case of parameter variations and fluctuations.

II. The Construction of Rotation Nonlinear Model for The PV Grid-connected Inverter

In the system analysis and controller design process of the three-phase converter, DQ rotating coordinate transformation which makes time-varying state variables becoming DC variables[18] is of great importance and commonly used. DQ transformation cannot be directly used for the single-phase converter owing to it requiring at least two orthogonal phase. In order to construct a single-phase converter orthogonal coordinate system, a virtual signal on the basis of the original signal is constructed to simulate the two-phase orthogonal signals to generate the DQ rotating coordinate system. The current building process illustrates the process of constructing orthogonal coordinate.

Assuming the actual steady-state current is

$$I_R = I_m \sin(\omega t + \theta), \tag{2.1}$$

where I_R is actual steady-state current, I_m is the peak value of the sinusoidal current, ω is frequency and $\theta$is initial phase of sinusoidal current. Ideally, the virtual orthogonal current is

$$I_I = I_m \cos(\omega t + \theta), \tag{2.2}$$

where I_I is virtual steady-state current.

The two-phase rotation coordinate system can be obtained in respect to the two-phase stationary coordinate system by using the transformation matrix of the formula (2.3).

$$T = \begin{bmatrix} \sin(\omega t) & \cos(\omega t) \\ -\cos(\omega t) & \sin(\omega t) \end{bmatrix}. \tag{2.3}$$

The current variable in DQ rotating coordinate system can be expressed as

$$\begin{bmatrix} I_D \\ I_Q \end{bmatrix} = T \begin{bmatrix} I_R \\ I_I \end{bmatrix} = I_m \begin{bmatrix} \cos\theta \\ \sin\theta \end{bmatrix}. \tag{2.4}$$

From (2.4), the AC variables after coordinate transformation become constants to simplify the analysis

and design of a controller.

The mathematical model of the typical single-phase photovoltaic grid-connected inverter in Fig1 based on the DQ rotating coordinate system is expressed as formula (2.5).

where

$u_{grid}=\begin{bmatrix} u_{dgrid} \\ u_{qgrid} \end{bmatrix}$, $i_{gc}=\begin{bmatrix} i_{dgc} \\ i_{qgc} \end{bmatrix}$, $u=\begin{bmatrix} u_d \\ u_q \end{bmatrix}$, $A=\begin{bmatrix} 1 \\ 0 \end{bmatrix}$, $M_P=\begin{bmatrix} 1 & 0 \\ 0 & 1 \end{bmatrix}$.

and V_{dc} is the dc bus voltage, C is the dc link capacitor, L_g is the inductance, R_g is the resistance of the inductance, u_{dgrid} , u_{qgrid} are the voltage of the grid in the d and q axes respectively, i_{dgc} , i_{qgc} are the current in the d and q axes respectively, u_d , u_q are the duty in the d and q axes respectively, τ is the sample time.

III. System Analysis and Optimal Controller Design

3.1 System Analysis

Inverter output current is the control object of Single-phase photovoltaic grid-connected inverter. It is hoped that the inverter can feed energy to the grid with unity power factor power or compensate the reactive power in rated power factor by controlling. In this paper, energy fed to the grid with unity power factor. Based on this, the controller objectives can be converted to the controlling of the DC bus voltage and reactive power feeding to the grid.

Reactive power can be determined [19] by the formula (3.1).

$$Q_{gc}(k)=\mathrm{u}_{grid}^{T}(k)\sqrt{i_{gc}(k)^2-(\frac{V_{pv}(k)I_{pv}(k)}{u_{grid}(k)})^2}, \quad (3.1)$$

where $u_{grid}(k)$, $i_{gc}(k)$ are the grid voltage and current, $V_{pv}(k)$, $I_{pv}(k)$ are the voltage and current of the photovoltaic panel.

The static stable value of the reactive power can be determined [20] by formula (3.2).

$$Q_{gc}^{ss}(k)=\frac{P_{gc}^{ss}(k)}{f_{ss}}\sqrt{1-f_{ss}^2}, \quad (3.2)$$

where $P_{gc}^{ss}(k)$ is active power, f_{ss} is power factor, $Q_{gc}^{ss}(k)$ is reactive power.

Thereby, the tracking error of the state variables can be obtained by formula (3.3).

$$\begin{cases} e_{V_{dc}}(k)=V_{dc}(k)-V_{dc}^{ss}(k) \\ e_{Q_{gc}}(k)=Q_{gc}(k)-Q_{gc}^{ss}(k) \end{cases}, \quad (3.3)$$

where V_{dc} is real-time state of the dc bus voltage, V_{dc}^{ss} is steady-state of the dc bus voltage, $e_{V_{dc}}$ is difference of the dc bus voltage, Q_{gc} is real-time state of reactive power, Q_{gc}^{ss} is steady-state of the reactive power, $e_{Q_{gc}}$ is difference of the reactive power.

Combining (3.1) - (3.3) with (2.5), the result is formula (3.4).

From (3.4), the current and DC bus voltage of steady-state operation can be obtained.

3.2 Optimal Controller Design

Once the optimal control applied to the system, it will bring significant results. Therefore, optimal control has been widely used in various fields.

Changing of state variables can reflect the effect of control, it is necessary to select the appropriate state variables as the control target. Combined with the system analysis in 3.1, the defined herein DC bus voltage and the current state of the target amount the synthesis of a new vector: $x(k)=[V_{dc}(k) \quad i_{dgc}(k) \quad i_{qgc}(k)]^T$, its corresponding steady state vector is: $x^{ss}(k)=[V_{dc}^{ss}(k) \quad i_{dgrid}^{ss}(k) \quad i_{qgrid}^{ss}(k)]^T$.

$$\begin{cases} V_{dc}(k+1)=V_{dc}(k)+\tau[\frac{1}{CV_{dc}(k)}u_{\mathrm{grid}}^{T}(k)M_P i_{gc}(k)] \\ i_{gc}(k+1)=i_{gc}(k)+\tau[-A\frac{V_{dc}(k)}{L_g}-\frac{R_g}{L_g}i_{gc}(k)+2\frac{V_{dc}(k)}{L_g}u(k)-\frac{u_{grid}(k)}{L_g}] \end{cases}, \quad (2.5)$$

$$\begin{cases} V_{dc}^{ss}(k)+\frac{\tau}{CV_{dc}^{ss}(k)}u_{grid}^{T}(k)M_P i_{gc}^{ss}(k)-V_{dc}^{ss}(k+1)=0 \\ \mathrm{u}_{grid}^{T}(k)\sqrt{i_{gc}^{ss}(k)^2-(\frac{V_{pv}(k)I_{pv}(k)}{u_{grid}(k)})^2}-\frac{u_{grid}^{T}(k)M_P i_{gc}^{ss}(k)}{f_{ss}}\sqrt{1-f_{ss}^2}=0 \end{cases}, \quad (3.4)$$

Thereby, the tracking error of the target can be expressed

$$\begin{cases} e_x(k)=x(k)-x^{ss}(k) \\ e_x(k+1)=x(k+1)-x^{ss}(k+1) \end{cases}. \quad (3.5)$$

In order to simplify representation of the system, using the synthetic vector to represent the definition of the formula (2.5), and the state variables can be expressed as

$$x(k+1)=f(\mathrm{x}(k))+g(\mathrm{x}(k))u(k)+h(k), \quad (3.6)$$

where

$$f(\mathrm{x}(k))=\begin{bmatrix} V_{dc}(k)+[\dfrac{\tau}{CV_{dc}(k)}u_{grid}^{T}(k)M_{P}i_{gc}(k) \\ -\dfrac{\tau A}{L_g}V_{dc}(k)+(1-\dfrac{\tau R_g}{L_g})i_{gc}(k) \end{bmatrix},$$

$$g(\mathrm{x}(k))=\begin{bmatrix} 0 & 0 \\ -\dfrac{2\tau}{L_g}V_{dc}(k) & 0 \\ 0 & -\dfrac{2\tau}{L_g}V_{dc}(k) \end{bmatrix},$$

$$h(k)=\begin{bmatrix} 0 \\ -\dfrac{\tau u_{grid}(k)}{L_g} \end{bmatrix}.$$

Combing (3.5) with (3.6) can get a new formula (3.7).

In order to improve control accuracy and effectiveness, the control variables are composed by steady-state variable and dynamic variable. Thereby, it is assumed that the formula (3.8) is established.

Substituting equation (3.8) into equation (3.7), then

$$e_x(k+1)=f(e_x(k))+g^{*}(e_x(k))u^{*}(k) \quad (3.9)$$

Since formula (3.9) is a typical nonlinear discrete affine system, the control method for nonlinear discrete affine system now can be used to design the controller.

Now, assume $u^{*}(k)=u_{ss}(k)+u_{dv}(k)$. In order to obtain and simplify the control goal, substitute it into the formula (3.7) and formula (3.8), then formula (3.10) can be obtained.

Now, the stead-state control variable can be got by formula (3.11).

Formula (3.9) can be expressed as follows

$$e_x(k+1)=f(e_x(k))+g^{*}(e_x(k))u_{dv}(k). \quad (3.12)$$

By the formula (3.12) it is clearly seen that the control model of the system is a non-linear discrete affine model. Therefore, with nonlinear discrete emission system control method, the meaningful cost functional is defined as [20]

$$V(e_x(k))=\sum_{n=k}^{\infty}(l(e_x(n)+u_{dv}(n)^{T}R(e_x(n))u_{dv}(n)), \quad (3.13)$$

where l is a positive semi-definite function with the same dimension of $x(k)$, R is a real symmetric positive definite weighting matrix with the same dimension of $u_{dv}(k)$. Then, the mathematical deformation of formula (3.13) can be expressed as formula (3.14).

If $V(0)=0$, then $V(e_x(k))$ becomes a Lyapunov function. It can be expressed as formula (3.15).

So,The derivation of formula (3.14) can obtain

$$2R(x(k))u_{dv}(k)+\frac{\partial V(e_x(k+1))}{\partial u_{dv}(k)}=0. \quad (3.16)$$

Combining with formula (3.12), $u_{dv}(k)$ can be expressed as formula (3.17).

For formula (3.17), it is difficult to solve Hamilton-Jacobi-Bellman. Therefore, based on the optimal control theory and References [21] a Lyapunov control function is constructed.

$$V(e_x(k))=\frac{1}{2}e_x{}^{T}(k)Pe_x(k), \quad (3.18)$$

where P is a real symmetric positive definite weighting matrix.

Now, the result of formula(3.17)can be expressed

$$e_x(k+1)=f(e_x(k))+f(\mathrm{x}^{ss}(k))+g(e_x(k)+\mathrm{x}^{ss}(k))u(k)+h(k)-x^{ss}(k+1). \quad (3.7)$$

$$g^{*}(e_x(k))u^{*}(k)=f(\mathrm{x}^{ss}(k))+g(e_x(k)+\mathrm{x}^{ss}(k))u(k)+h(k)-x^{ss}(k+1). \quad (3.8)$$

$$\begin{cases} f(\mathrm{x}^{ss}(k))+g(e_x(k)+\mathrm{x}^{ss}(k))u_{ss}(k)+h(k)-x^{ss}(k+1)=0 \\ g^{*}(e_x(k))=g(e_x(k)+\mathrm{x}^{ss}(k)) \end{cases}. \quad (3.10)$$

$$u_{ss}(k)=(g(e_x(k)+\mathrm{x}^{ss}(k)))^{-1}(-f(\mathrm{x}^{ss}(k))-h(k)+x^{ss}(k+1)). \quad (3.11)$$

$$V(e_x(k))=l(e_x(k)+u_{dv}(k)^{T}R(e_x(k))u_{dv}(k)+V(e_x(k+1)). \quad (3.14)$$

$$V(e_x(k))=\min_{u(k)}\{l(\Delta x(k)+u_{dv}(k)^{T}R(e_x(k))u_{dv}(k)+V(e_x(k+1))\}. \quad (3.15)$$

$$u_{dv}(k)=-\frac{1}{2}R^{-1}(e_x(k))g^{*T}(e_x(k))\frac{\partial V(e_x(k+1))}{\partial e_x(k+1)}. \quad (3.17)$$

$$u_{dv}(k)=-\frac{1}{2}(R(e_x(k)))^{-1}(I+\frac{1}{2}R(e_x(k))g^{*T}(e_x(k))Pg^{*}(e_x(k)))^{-1}\,g^{*T}(e_x(k))Pf(e_x(k)). \quad (3.19)$$

as formula (3.19).

IV. Simulation Works

In order to verify the characteristics of the designed controller, the controlling system will be simulated in MATLAB. From the design results of the optimal controller, only P is unknown. This paper takes an empirical value by a large number of experimental verification, and it must be a positive semi-definite weighting matrix in order to meet the stability of the

controller.

In this paper, we set the dc bus voltage V_{dc} is $40V$ and the RMS voltage of the grid is $22V$ which are ten percentage of the nominal voltage of $220V$ power system. To illustrate the wide stability margin of the controller and less demanding on system parameters characteristic, four simulates are given. The first simulation parameters of the system are: dc link capacitor C is 4700 μF , the inductance L_g is 1 mH , the resistance of the inductance R_g is 0.47 Ω , and the switching frequency is 50 KHz .

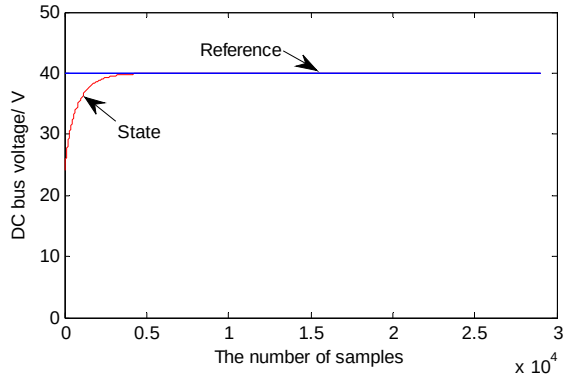

(a)The Response Curve of DC bus voltage

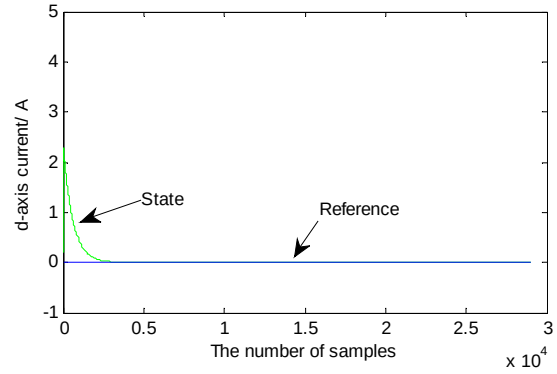

(b)The Response Curve of d axis current

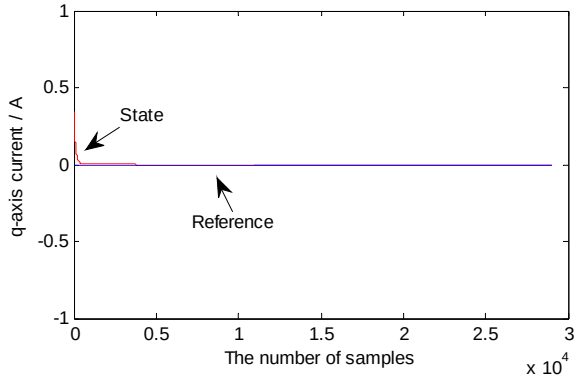

(c)The Response Curve of q axis current

Fig 2 Variable response curves of the system in first simulation parameters

Dynamic tracking of the DC bus voltage response curve is shown in figure 2(a). Wherein the red means the dynamic tracking state values, and blue indicates its reference value. Since there is no load in the system, so its d axis reference current is set to 0, In order to ensure the unity power factor, the q axis current reference value is also set to 0 apparently. Thus, the dynamic current tracking response curve of d axis and q axis are shown in figure 2(b) and figure 2(c) ,Similarly.

In order to verify the impact of inductance parameter changing on the controller, the second simulation parameters are set as: dc link capacitor C is 4700 μF , the inductance L_g is 2 mH , the resistance of the inductance R_g is 0.6 Ω , and the switching frequency is 50 KHz .

Similarly, Dynamic tracking of the DC bus voltage response curve and the dynamic current tracking response curve of d axis and q axis are shown in figure 3(a), 3(b) and 3(c).

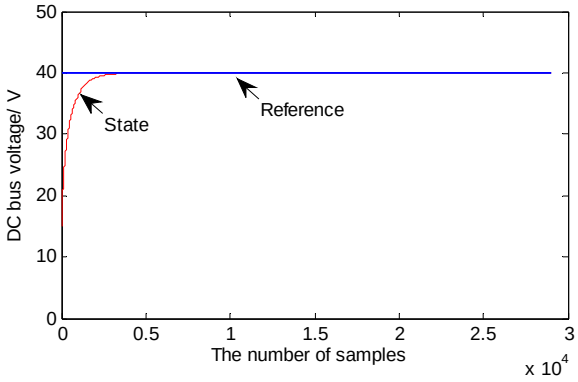

(a)The Response Curve of DC bus voltage

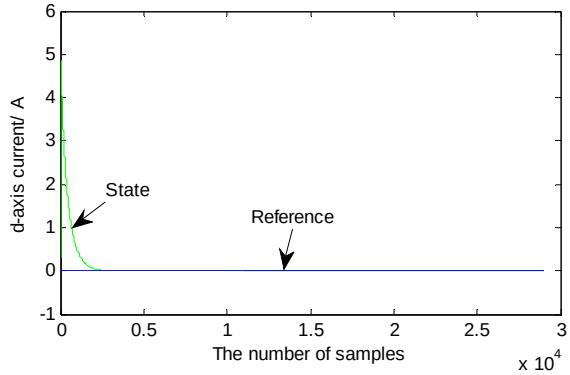

(b)The Response Curve of d axis current

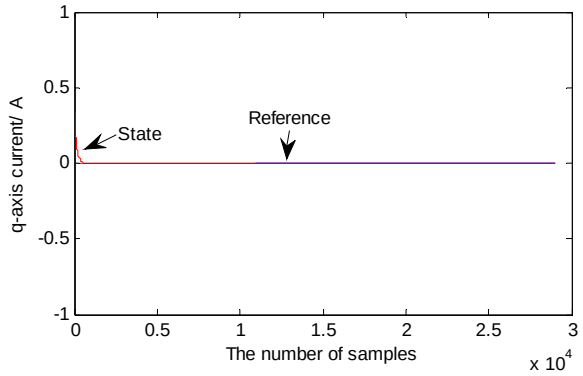

(c)The Response Curve of q axis current

Fig 3 Variable response curves of the system in inductor parameter changing

In order to verify the impact of capacitor parameter changing on the controller, the third simulation parameters are set as: dc link capacitor C is 6800 μF, the inductance L_g is 1 mH, the resistance of the inductance R_g is 0.47 Ω, and the switching frequency is 50 KHz.

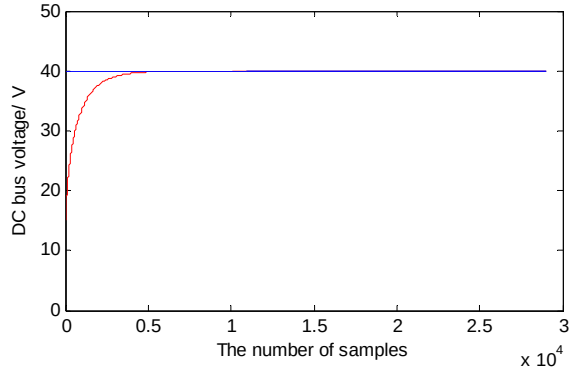

(a)The Response Curve of DC bus voltage

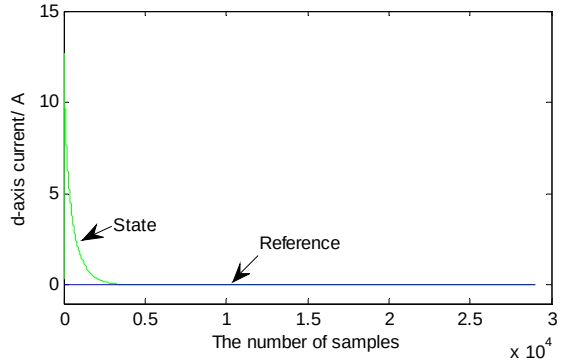

(b) The Response Curve of d axis current

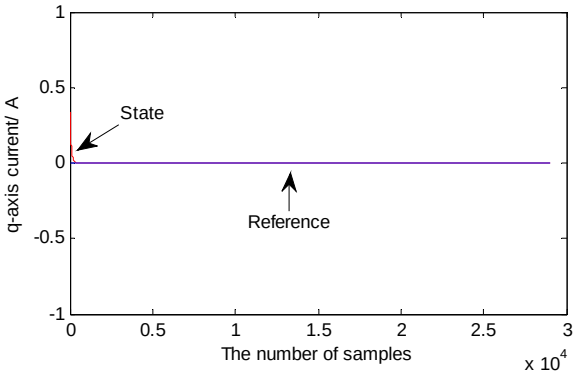

(c)The Response Curve of q axis current

Fig 4 Variable response curves of the system in capacitor parameter changing

Similarly, Dynamic tracking of the DC bus voltage response curve and the dynamic current tracking response curve of d axis and q axis are shown in figure 4(a), 4(b) and 4(c).

In order to verify the impact of synthesized parameters changing on the controller, the fourth simulation parameters are set as: dc link capacitor C is 6800 μF, the inductance L_g is 2.2 mH, the resistance of the inductance R_g is 0.3 Ω, and the switching frequency is 40 KHz.

Similarly, Dynamic tracking of the DC bus voltage response curve and the dynamic current tracking response curve of d axis and q axis are shown in figure 5(a), 5(b) and 5(c).

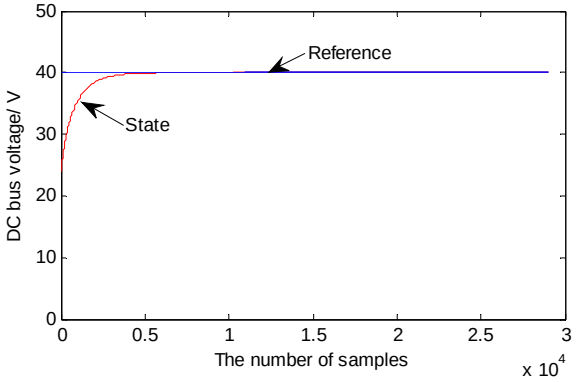

(a)The Response Curve of DC bus voltage

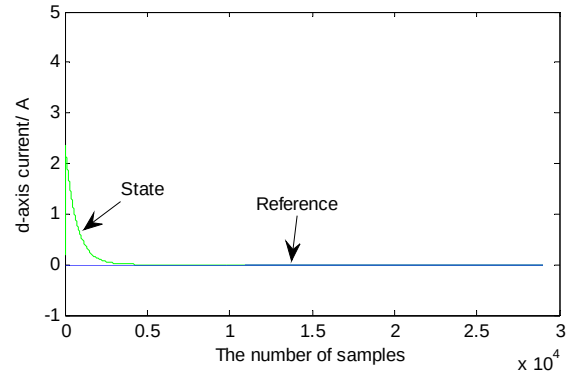

(b) The Response Curve of d axis current

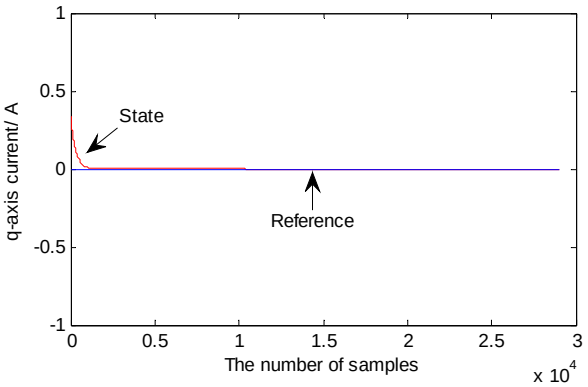

(c)The Response Curve of q axis current

Fig 5 Variable response curves of the system in synthesized parameters changing

As can be seen from figure 2, figure 3, figure4 and figure 5, the controller can eliminate static error and has a good dynamic response. Comparing figure 2 with figure 3, it confirms that the controller has strong robustness to the changing parameter. Similarly, figure 4 and figure 5 also prove this problem. In summary, the controller has less weak dependence on the system parameters and it has strong robustness.

V. Conclusion

Against the problems of existing grid-connected photovoltaic inverter control methods, in this paper we have proposed an optimal control method which is effective to eliminate static error of the system and has a good dynamic response. In addition, the nonlinear model of the single-phase grid-connected photovoltaic inverter was also constructed based on the rotating coordinate system which implements the active and reactive power decoupling. Using the optimal control method can avoid low performance of the traditional linear and nonlinear methods. Simulation results show that the controller is good at eliminating static error and has better dynamic and static characteristics, and it has stronger robustness to the parameters changing of the system.

Acknowledgment

This work was supported by the National Natural Science Foundation of China (61273029,61273027) and the Program for New Century Excellent Talents in University, China(NCET-12-0106).

Reference

[1] Blaabjerg. F, Iov. F, Kerekes. T,et al. “Trends in Power Electronics and Control of Renewable Energy Systems”. 14th International Power Electronics and Motion Control Conference (EPE/PEMC), 2010, pp. 1-19.

[2] Q. Mei, M. Shan, et al. “A Novel Improved Variable Step-Size Incremental-Resistance MPPT Method for PV Systems”. IEEE Transactions on Industrial Electronics, vol.58, no.06, 2011, pp. 2427-2434.

[3] Junyin Gu, Guocheng Chen. “A current-sensor-less MPPT Algorithm for Single-stage Grid-connected PV Inverters”. Proceedings of the CSEE, vol.32, no.27, 2012, pp.149-153.

[4] N. Femia, G Petrone, G Spagnuolo. “Optimization of perturb and observe maximum power point tracking method”. IEEE Transactions on Power Electronics, vol.20, no.04, 2005, pp. 963-973.

[5] Esram T,Chapman P L. “Comparison of photovoltaic array maximum power point tracking techniques”. IEEE Transactions on Energy Conversion, vol.22, no.02, 2007, pp. 439-449.

[6] Yuliang Chen,Weixin Xu. “SPWM single-input single-phase modulation of photovoltaic power generation system and network modulation control law studies”. Solar Journal, vol.25, no.06, 2004, pp.794-798.

[7] Qinglin Zhao, Xiaoqiang Guo, Weiyang Wu. “Research on Control Strategy for Single-Phase Grid-connected Inverter”. Proceedings of the CSEE, vol.27, no.16, 2007, pp. 60-64.

[8] Teodorescu R,Blaabjerg F,Liserre M,et al. “Proportional resonant controllers and filters for grid-connected voltage-source converters”. IEE Proceedings of Electric Power Application, vol.153, no.05, 2006,pp.750-762.

[9] Wei Yao, Min Chen, Shanke Mou, et al. “Digital Control Method for High-performance Inverters Based on Feedback Linearization”. Proceedings of the CSEE, vol.30, no.12, 2010, pp. 14-19.

[10] Dingxin Shuai, Yunxiang Xie, Jingming Yang, et al. “Optimal control of Single-Phase Full-Bridge Inverters by State Feedback Linerarization”. Proceedings of the CSEE, vol.21, no.11, 2009, pp.120-126.

[11] Kun Mu,Xiaoyu Ma,Xiaobin Mu. “A New Nonlinear Control Strategy for Three-Phase Photovoltaic Grid-connected Inverter”. International Conference of Electronic and Mechanical Engineering and Information Technology(EMEIT), 2011, pp.4611-4614.

[12] Hao Ma, Fei Xu, Li Du. “Discrete-Time Passivity-Based Sliding-Mode Control of Single-Phase Current-Source Inverter”. Industrial Electronics, IECON '09. 35th Annual Conference of IEEE, 2009, pp. 403-407.

[13] Geng Pan, Wu Weimin, Ye Yinzhong, et al. “Single-Phase Time-Sharing Cascaded Photovoltaic Inverter Based on Repetitive Control”. Transactions of China Electronic technical Society, vol.26, no.03, 2011, pp. 116-122.

[14] C. Meza, D. Biel, D. Jeltsema. “Lyapunov-Based Control Scheme for Single-Phase Grid-Connected PV Central Inverters”. IEEE Transactions on control systems technology, vol.20, no.02, 2012, pp.520-529.

[15] Dingxin Shuai, Yunxiang Xie, Xiaogang Wang. “Optimal Control of Buck Converter by State Feedback Linearization”. Proceedings of the CSEE, vol.28, no.33, 2008, pp. 1-5.
[16] Majid Pahlevaninezhad, Pritam Das, Josef Drobnik, et al. “A Nonlinear Optimal Control Approach Based on the Control-Lyapunov Function for an AC/DC Converter Used in Electric Vehicles”. IEEE Transaction on Industrial Informatics, vol.08, no.03, 2012, pp. 596-614.
[17] Wang Jun, Ji Haibo, Xi Hongsheng, et al. “Adaptive Inverse Optimal Control for Strict-feedback Nonlinear Systems”. Journal of University of Science and Technology of China, 2002,32(6):713-719.
[18] Meiqin Mao, Li Yu, Bin Xu, et al. “Research of D-Q Control and Simulation for Single Phase Current Source Inverters”. Journal of System Simulation, vol.23, no.12, 2011, pp. 2727-2731.
[19] Shuangjian Peng, An Luo, Fei Rong, et al. “Single-phase Photovoltaic Grid-connected Control Strategy With LCL Filter”. Proceedings of the CSEE, vol.32, no.21, 2011, pp.17-24.
[20] Guangru Zhang, Dongsheng Yang, Ting Liu, et al. “Grid-connected of Photovoltaic Module Using Inverse Optimal Control”. 2013 International Conference on Computer Science, Electronics Technology and Automation, in press.
[21] Riemann Ruiz-Cruz, Edgar N. Sanchez, Fernando Ornelas-Tellez, et al. “Particle Swarm Optimization for Discrete-Time Inverse Optimal Control of a Doubly Fed Induction Generator”. IEEE Transactions on Cybernetics, vol.43, no.02, 2012, pp. 1-12.

Guangru Zhang was born in Gansu, China, in 1989. He received the Bachelor’s degree in Electrical Engineering and Automation in 2012, from Northeastern University, Shenyang, China. He is currently completing the Master’s degree in Electrical Engineering, from Northeastern University, Shenyang, China. He research interests include automation of power system, control of grid-connected new energy, and intelligent control.

Dongsheng Yang was born in Liaoning, China, in 1977. He received the Bachelor’s degree in Measurement and Control Technology and Instrument Specialty in 1999, from Northeastern University, Shenyang, China. He received the Master’s degree in Power Electronics and Electrical Drive in 2004, from Northeastern University, Shenyang, China. He received the Doctor’s degree in Control theory and control engineering in 2007, from Northeastern University, Shenyang, China. He is currently a professor of College of Information Science, Northeastern University, Shenyang, China. He research interests include automation of power system, control of grid-connected new energy, and intelligent control.

Ting Liu was born in Liaoning, China, in 1981. He received the Bachelor’s degree in Agricultural Electrification and Automation in 2004, from Shenyang Agricultural University, Shenyang, China. He received the Master’s degree in Computer Technology in 2010, from Northeastern University, Shenyang, China. He is currently an assistant engineer of Yuhong Power Supply Bureau of Shenyang Power Supply Company, Shenyang, China. He research interests include automation of power distribution, control of grid-connected new energy, and power demand side management.

Bo Hu was born in Liaoning, China, in 1972. He received the Bachelor’s degree in Computer and Its Applications in 1995, from North China Electric Power University, Beijing, China. He received the Master’s degree in Computer Technology in 2006, from North China Electric Power University, Beijing, China. He is currently a senior engineer of Liaoning Electric Power Company Limited, Shenyang, China. He research interests include marketing of power system and charging for electricity of electric vehicle.